



Spatial Variations in Groundwater-Surface Water Interactions at the Basin Scale of an Arid Region: Insights from Stable Isotopes and Hydrochemistry

Liheng Wang^{1,2}, Yuejia Sun^{1,2}, Chun Yang³ Yanhui Dong^{1,2}

¹ State Key Laboratory of Deep Petroleum Intelligent Exploration and Development, Institute of Geology and Geophysics, Chinese Academy of Sciences, Beijing 100029, China

² College of Earth and Planetary Sciences, University of Chinese Academy of Sciences, Beijing 100049, China

³ School of Geophysics and Information Technology, China University of Geosciences (Beijing), Beijing 100083, China

Correspondence to: Yanhui Dong (dongyh@mail.iggcas.ac.cn)

Abstract. A comprehensive understanding of groundwater-surface water interaction patterns is crucial, particularly in arid regions of Central Asia, where typical river-groundwater systems are prevalent. In this study, 31 river water and groundwater samples were collected from the Shule River Basin (SRB) in Northwest China and analysed for hydrochemical and stable isotopic characteristics to elucidate spatial variations in groundwater-surface water interactions. A notable finding is the significant negative correlation between the $\delta^{18}\text{O}$ of river water and elevation, with a vertical lapse rate of 0.08‰/100 m, which is markedly lower than that observed in the adjacent Qinghai-Tibet Plateau. Isotopic analysis indicates that groundwater recharges river water in the upper reaches, while river water recharges groundwater in the lower reaches, highlighting a basin-scale transformation in their relationship. Hydrochemical analysis reveals that river water has an average pH of 8.36 and a mean TDS of 649.93 mg/L, while groundwater shows an average pH of 7.65 and a mean TDS of 759.13 mg/L. Both river water and groundwater exhibit increasing TDS from upstream to downstream, transitioning from slightly hard to hard water, yet both are suitable for irrigation. The chemical composition of river water is primarily influenced by silicate and carbonate weathering, whereas groundwater chemistry is dominated by mineral dissolution and ion exchange processes. This study provides critical insights into basin-scale hydrological cycles in Central Asia's arid regions, offering valuable guidance for the sustainable management of groundwater resources in semi-arid environments.

1 Introduction

Arid and semi-arid regions, which cover more than 40% of the global land area, support approximately 38% of the world's population (Jasechko and Perrone, 2021; Wang et al., 2023). Water resources management in this region is facing increasing challenges under pressure from climate changes and socio-economic needs, such as increasing population numbers, expanding areas of irrigated agriculture, and growing industrial demands. Discerning the origins and water quality evolution processes of various waters establishes a fundamental foundation for achieving sustainable water development and equitable resource allocation. (Banerjee and Ganguly, 2023; Crosbie et al., 2023; Wang et al., 2015; Wang et al., 2022). However, due to



constraints such as arid climate and measurement accuracy, traditional hydrological survey and research methods face significant challenges in achieving this objective. As natural tracers, the stable hydrogen and oxygen isotopes (2H , 18O) in water, along with its hydrochemical composition, are widely employed to trace sources and analyze evolutionary processes (Cocca et al., 2023; Guidah Chabi et al., 2023; Herrera et al., 2023; Négrel et al., 2003). Normally the isotopic method is
35 complemented by additional determination of major cations and anions in the same samples.

Currently, isotopic characteristics and hydrochemical composition of river water and groundwater are frequently utilized to unravel the origins of water, conduct water quality assessments, and analyze the interaction between river water and groundwater (Aravena et al.; Glok-Galli et al., 2022; Herczeg and Leaney, 2011; Négrel et al., 2003; Prakash Rai et al., 2023; Xie et al., 2024; Yang et al., 2021; Yin et al., 2021). Considering the elements potentially involved in the hydrologic cycle
40 process, factors like the hydrochemical composition of rainwater, the distribution of surface rocks in the watershed, and the mineralogical composition of the aquifers all influence the quality of river water and groundwater. This influence is particularly pronounced in arid regions due to highly intense evaporation. Furthermore, human activities, such as domestic water usage, industrial production, and agricultural irrigation, also contribute to deteriorating water quality. Given the multitude of factors at play, numerous major rivers worldwide, such as Yellow River (Kuang et al., 2019), Yangtze River (Guo et al., 2023; Herath
45 et al., 2019), Mississippi River (Cai et al., 2020), Amazon River (da Cunha and Sternberg, 2018), Indus River (Rehman Qaisar et al., 2018), Yarlung Tsangpo river (Li et al., 2021; Qu et al., 2017), have undertaken studies on the chemical composition and isotopic characteristics to elucidate the mechanisms controlling water quality in recent years (Hamidi et al., 2023). In addition, an increasing number of environmental isotopes, such as sulfur (Xie et al., 2022), strontium and uranium (Paces and Wurster, 2014), are being introduced to analyze the conversion relationship between groundwater and surface water, and in
50 order to quantify the interactions between them, numerical simulations also have been adopted to carry out their studies (Jafari et al., 2021). In contrast, due to the scarcity of water resources, conducting similar studies in arid regions have attracted more attention (Wang et al., 2023; Wu et al., 2020).

The Shule River basin (SRB), located in the hyper-arid and arid northwest region of China, is not only historically significant as part of the ancient Silk Road but also renowned for its numerous oases that serve as the basis of local livelihoods and
55 economic development (Yang et al., 2020b). Therefore, regional water resources are not only vital for sustaining local socio-economic growth but also crucial for safeguarding the delicate ecosystems. In the upper reaches of the Shule River are the ecologically fragile Qilian Mountains on the northern edge of the Qinghai-Tibet Plateau. Zhou et al. (2015) attempted to study the characteristics of rainwater, glacial water, groundwater and river water using isotopic techniques, and initially concluded that in the upstream area groundwater is the main source of river water recharge. Similarly, Wang et al. (2016) also utilized an
60 isotopic approach to analyze the interaction between surface water and groundwater in the lower reaches of the Shule River, and concluded that agricultural irrigation water from the river is an important source of groundwater. In addition, Xie et al (2022, 2024) meticulously examined the hydrochemistry and multi-isotope composition of river and groundwater within the SRB, and preliminarily analyzed the sources of substances in the water. Recognizing the importance of water resources in this region, extensive studies have been conducted through various approaches and methodologies over the years. While previous



65 research has focused on specific agricultural irrigation areas, others have targeted the origins and evolution of groundwater (Guo et al., 2015; He et al., 2015; Wang et al., 2015). Nevertheless, it needs to be emphasized that there is an urgent need to clarify the process of river-groundwater interactions at the basin scale and to systematically present the water quality characteristics to provide insights for sustainable management of regional water resources.

Consequently, this study aims to achieve several objectives by analyzing the chemical composition and isotopic characteristics
70 of the mainstream water and the groundwater samples from the SRB: 1) to elucidate the isotopic and hydrochemical compositions of both river water and groundwater; 2) to clarify the transformation processes between these water sources in the basin scale; and 3) to establish fundamental water quality characteristics for the SRB, which will have implications for various water resource applications, including agricultural irrigation and human and livestock consumption. By gaining a comprehensive understanding of the interaction between groundwater and river water, as well as the mechanisms governing
75 water quality, this research seeks to provide a valuable set of scientific data for the development and utilization of water resources in the SRB.

2 Materials and methods

2.1 Study area description

The SRB is geographically located on the northern edge of the Qinghai - Tibet Plateau, in northwestern China. It is bordered
80 by longitude 92°11' to 98°30' E and latitude 38°00' to 42°48' N. The mainstream of the Shule River is more than 620 km, covering a drainage area exceeding 40,000 km². Its mainstream origin can be traced back to a network of 347 glaciers nestled in the western section of the Qilian Mountains. Flowing in a northwest direction, the mainstream of the Shule River meanders through many gorges in the Qilian Mountains (Fig. 1), before flowing into the Changma basin. After the Shule River flows out of the Qilian Mountains at the Changma Reservoir, it flows from east to west along the edge of the alluvial fan through
85 Yumen, then enters the Shuangta Reservoir, continues to flow west through Guazhou, and finally disappears in the Kumtag Desert. Therefore, it can be divided into three distinct segments, each characterized by its unique geographical features. The upper reaches, stretching from the river's source to the outlet of the Changma Reservoir (Fig. 1), lie at elevations ranging from 2080 to 5808 m, with an average elevation of 3944 m. This region is primarily dominated by towering and precipitous mountain formations, interspersed with relatively gentle valleys, particularly in the vicinity of Changma. Progressing further downstream,
90 the middle reaches encompass the vast expanse of the Yumen Alluvial Fan Plain (Fig. 1). With elevations fluctuating between 1310 to 2050 m, this segment of the river exhibits a notable decrease in altitude from south to north. Finally, the lower reaches of the Shule River encompass the extensive Guazhou Plain, abutting the northern mountainous region of the arid Gobi Desert, with elevations varying from 1020 to 1650 m. Therefore, the upstream region is primarily located in the high-altitude Qilian Mountains, while the midstream and downstream regions are situated in the relatively flat terrain of the Hexi Corridor (Fig.
95 1).

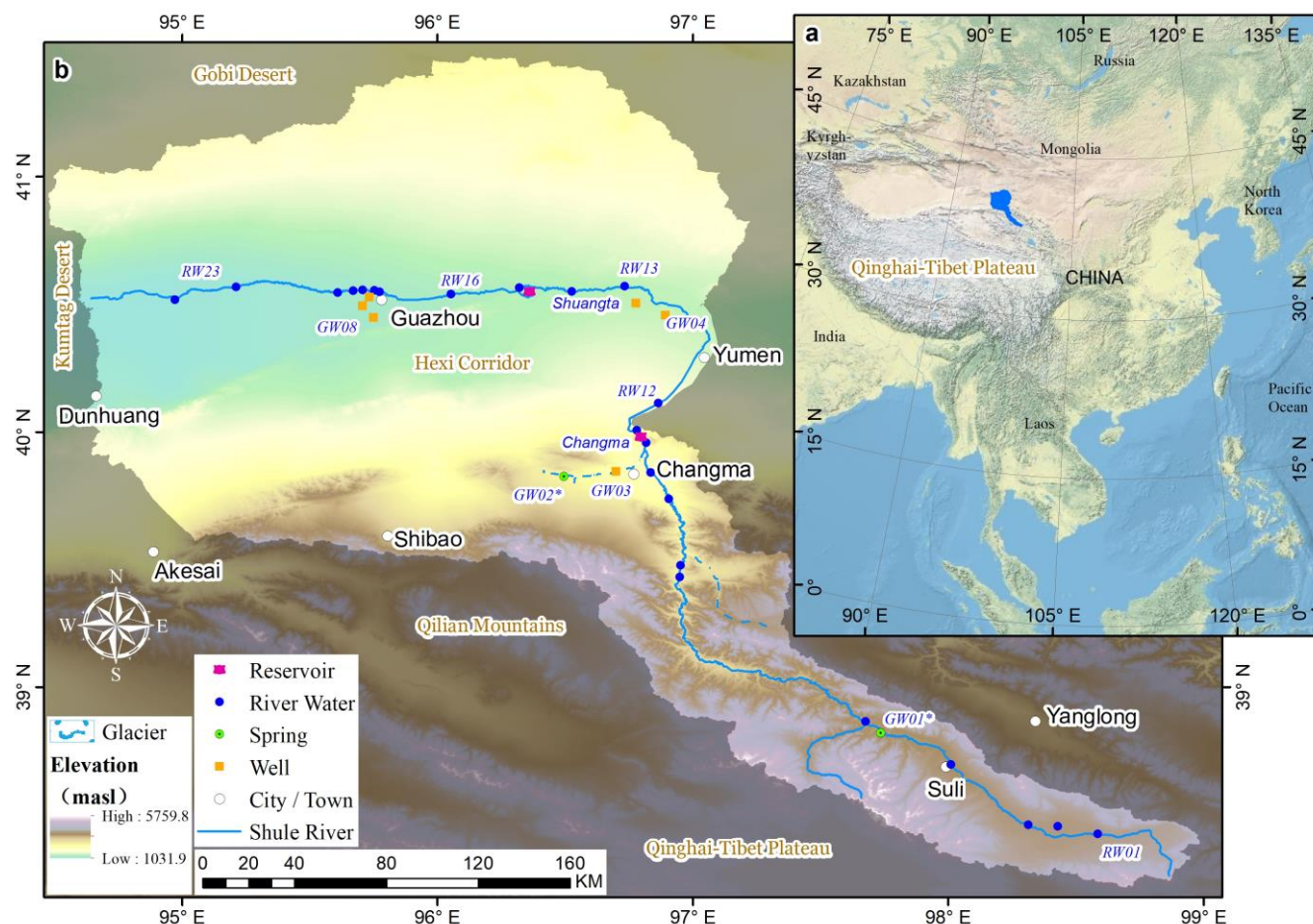


Figure 1 (a) Geographic location of the study area (Data Source: USGS). (b) Sampling sites for river water, groundwater across Shule River Basin.

As for the sources of recharge for the Shule River's flow, they encompass various crucial elements, such as the meltwater from glaciers, groundwater reserves, and localized precipitation. However, the average annual runoff of the mainstream, which amounts to $10.31 \times 10^8 \text{ m}^3$, undergoes a gradual decline as the river enters the Hexi Corridor. This decline is largely attributed to the heightened exploitation and utilization of water resources due to agricultural irrigation and industrial production, leading to a higher rate of evaporation and seepage losses.

The study area is situated in the heartland of the Eurasian continent, far from the influence of oceans, resulting in an extremely dry climate. The region is characterized by scarce precipitation and intense evaporation. The SRB, on average, receives a meager annual precipitation of 78.5mm, while the evaporation rate is remarkably high at 3042mm. The annual average temperature ranges from 6.9 to 8.8°C. The southern part of the study area, which encompasses the Qilian Mountain range, belongs to a high-altitude semi-arid climate zone, with precipitation levels ranging from 100 to 200mm and occasionally reaching up to 400mm. The temperatures in this area remain cold, hovering between 0 to 4°C, with an annual evaporation of



about 1700mm. Conversely, the middle and lower reaches of the basin fall within a temperate arid zone, receiving an even more limited annual precipitation ranging from 36 to 63mm. The average temperatures here range from 6 to 8°C, and the evaporation rates vary between 1500 to 2500mm annually.

2.2 Geology and hydrogeology setting

The study area is situated within a highly tectonically active region in the northern part of the Qinghai-Tibet Plateau. It is characterized by intense geological processes, including thrust faults and structural uplift. Qilian Mountains, which has experienced significant uplift since the late Paleozoic, it is subjected to a prominent NNE-directed compressional tectonic force (Lin et al., 2022; Yang et al., 2020a). This force has led to the formation of a series of NNE trending faults (Fig. 2), which play a crucial role in shaping the development of the Shule River system.

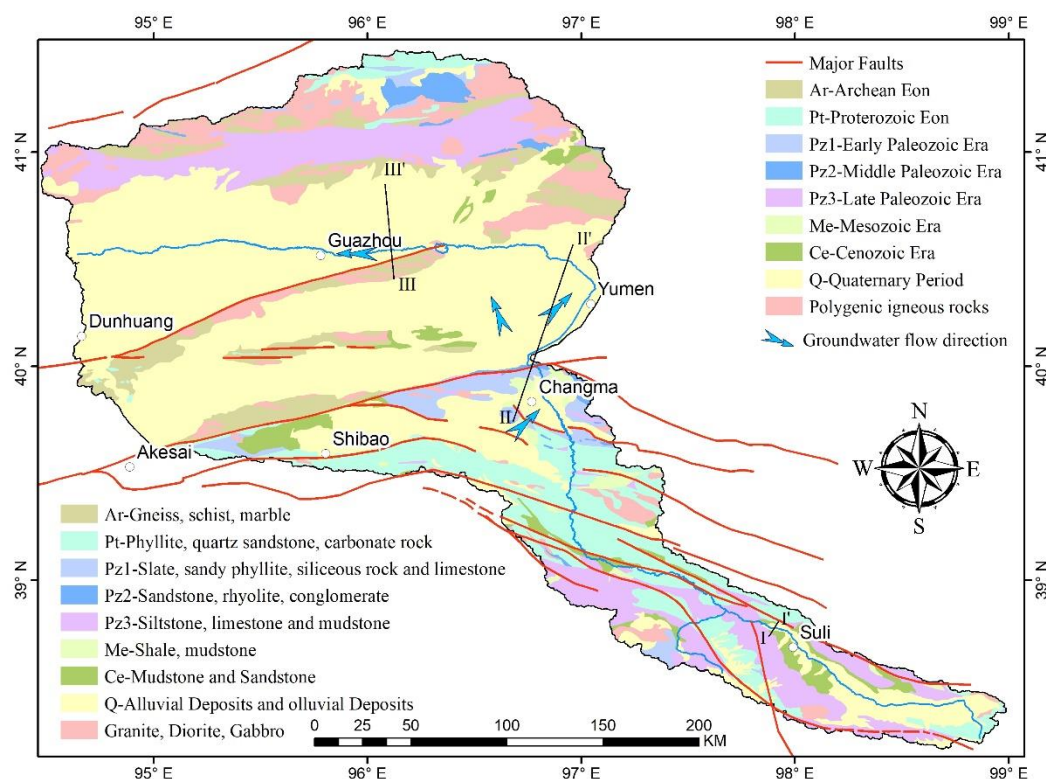


Figure 2 Geological, structural and hydrogeological maps of the study area.

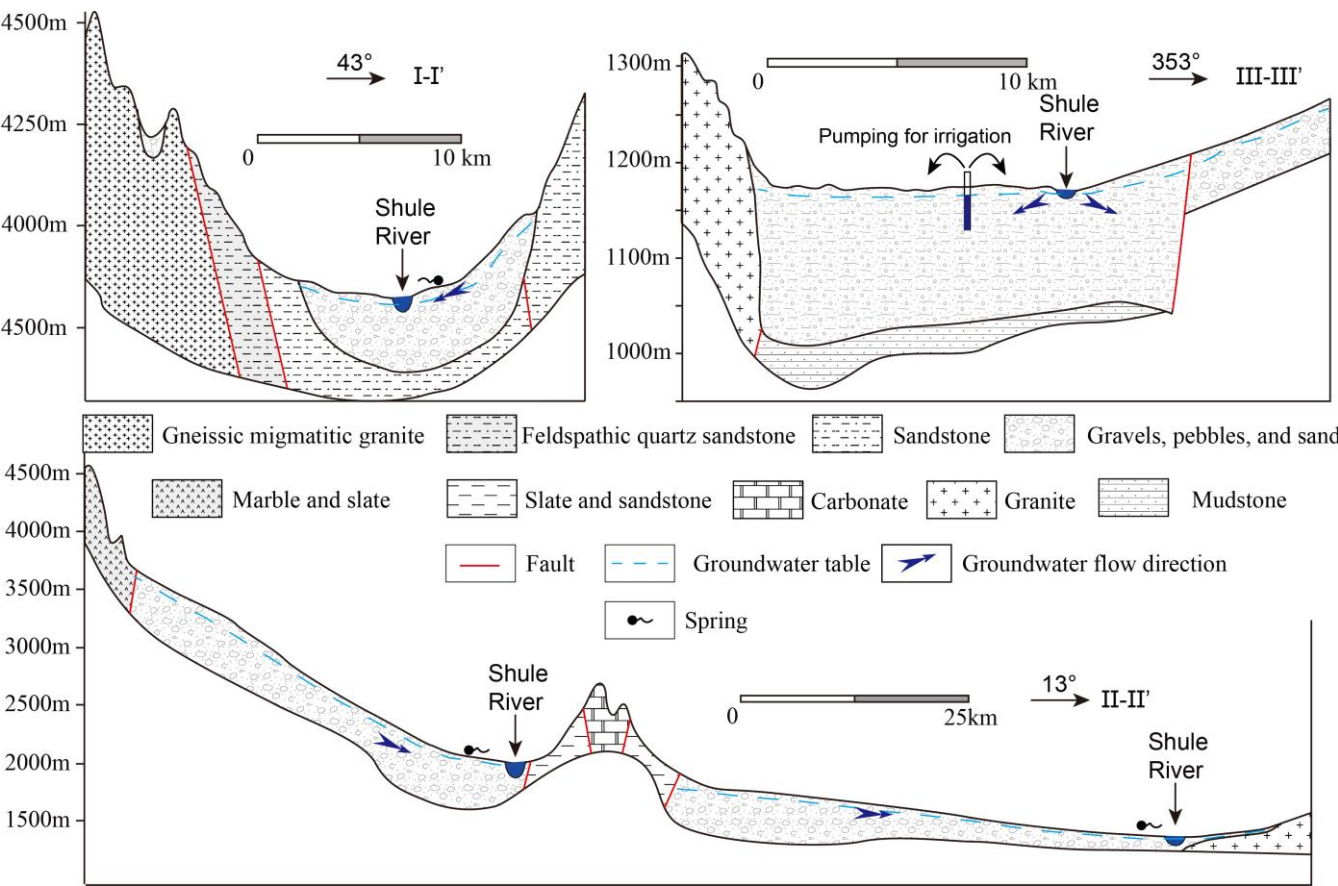
The upstream region of the Shule River is extensively covered with various rock types (metamorphic, sedimentary rocks) spanning multiple geological periods (Fang et al., 2005; Li et al., 1999). This includes Precambrian metamorphic rocks such as gneiss, schist, dolomite, and quartzite, as well as early Paleozoic metamorphic rocks like slate, sandstone, conglomerate, and carbonate rocks. Additionally, sedimentary rocks and granitic formations from different geological stages are also present. Furthermore, in the upstream area, sedimentary rocks dating back to the Mesozoic and Late Paleozoic periods, including



sandstones, mudstones, and limestones, can be observed. Throughout the Mesozoic era, the Hexi Corridor gradually took shape and experienced significant subsidence (Meng et al., 2020; Zhao et al., 2001). As it entered the Cenozoic era, the Qilian Mountains region underwent extensive erosion. Rivers transported substantial quantities of debris into the Hexi Corridor, leading to the deposition of thick Quaternary sediments. Over time, this process gave rise to various-sized alluvial fans.

130 Quaternary sediments constitute a significant component of the stratigraphy in the foreland alluvial fans and basins of the study area. These unconsolidated fluvial deposits, which include loess, gravel, and sand, can reach a thickness of 500 to 600 meters in the middle to upper reaches of the Shule River. Examples of such deposits can be observed in the Changma alluvial fan and the Yumen alluvial fan in the upper and middle reaches, respectively (Wang et al., 2017, Guo et al., 2015).

Groundwater with water supply significance in the study area is distributed in the alluvial fan plain area or on both sides of the river valley. These groundwaters exist in the pore of the Quaternary loose sediments. Previous studies have indicated that the primary source of recharge for groundwater is atmospheric precipitation, and its flow direction is intimately tied to the local topography (Fig. 2) (Guo et al., 2015). Because river water and groundwater have undergone many mutual transformations from upstream to downstream, it is believed that there is a close hydraulic connection between the two (He et al., 2015; Wang et al., 2016; Xie et al., 2022). In the upper reaches, because it is mostly mountains and canyons, the terrain changes very
140 drastically, so scattered springs are found. In the alluvial-diluvial fan edge area, groundwater flow is impeded, giving rise to the emergence of artesian springs. This phenomenon is frequently observed in the peripheries of the Changma and Yumen alluvial fan plains. Similar to other foreland alluvial fans, the sediments are coarse-grained at the mouths of the Changma and Yumen fans but become relatively fine-grained at the edges. This depositional pattern significantly influences the spatial distribution of groundwater within these alluvial fans. In particular, in both Changma and Yumen, the aquifer systems transition
145 from a single unconfined layer in the southern regions to multiple, interlayered confined layers towards the northern regions. Therefore, the thickness of the aquifers also varies significantly in space, ranging from tens to hundreds of meters. Correspondingly, the groundwater depth also varies, ranging from several meters to several hundred meters (Fig. 3, Wang et al., 2016, 2017).



150 **Figure 3: Hydrogeological cross-sections of upper, middle and lower reaches of the Shule River, and their location were indicated in Fig. 2. These cross-sections were adapted from the regional hydrogeological atlas of the study area (Gansu Geology Survey 1978~1980).**

2.3 Sample Collection and Analysis

In July 2022, a total of 31 sample sets were collected within the study area. These samples consisted of 23 river water samples and 8 groundwater samples (including both spring and well water). The distribution of samples is illustrated in Fig. 1.

For river water sample collection, efforts were made to select locations situated away from the riverbed, and samples were collected from a depth of 10 cm below the water surface at flowing sections of the river. When conducting groundwater sampling, spring water samples are typically collected directly from the spring source, capturing fresh groundwater immediately upon its emergence. Well water samples are obtained from agricultural irrigation wells within the study area. To ensure the representativeness of these samples, the wells were generally pumped for three times the well volume before sample collection. According to field investigations conducted during sampling, the depths of these agricultural irrigation wells range from 80 meters to 200 meters. To enhance the water supply capacity of the wells, intake screens are installed along their entire lengths. All sample collection was conducted in a single round.



All samples underwent on-site filtration using 0.45-micron cellulose acetate filter membranes. They were then carefully stored in pre-cleaned polyethylene bottles, which had been rinsed three times with water from the respective sampling site. Three bottles were collected for each sample: one was acidified to a pH below 2 for cation testing, while the other two were designated for anion and stable isotope analysis. Throughout transportation to the laboratory, the water samples were stored at a constant temperature of 4 °C.

On-site measurements included pH, temperature, TDS (HANNA HI 9811-5), latitude and longitude coordinates of the sampling locations, as well as elevation. HCO_3^- was determined using a titration method, while all other cations, anions, and stable isotopes were comprehensively analyzed by the Weathering and Hydro-geochemistry Laboratory at the Institute of Geology and Geophysics, Chinese Academy of Sciences. The stable isotopes (D, ^2H and ^{18}O) in the water samples were analyzed using an L1102-I (Picarro, USA) and the results were expressed as delta values, defined as the per mil deviation from Vienna Standard Mean Ocean Water, as shown in Eq. 1. For precision, each sample is tested six times, with the first two measurements discarded, and the average of the remaining four used as the final value.

$$\delta = \frac{R_{\text{sample}} - R_{\text{standard}}}{R_{\text{standard}}} \times 1000, \quad (1)$$

where R represents the isotopes ratios ($^2\text{H}/^1\text{H}$ or $^{18}\text{O}/^{16}\text{O}$) of the sample and standard, respectively. The deuterium excess value can be calculated according to Dansgaard (1964).

2.4 Water quality for drinking and irrigation evaluation

The study area is a major agricultural irrigation region in the northwest of China, known as the part of the Hexi Corridor. Both surface water and groundwater play a crucial role in agricultural irrigation and drinking water. In order to assess the quality of irrigation water versus drinking water, Sodium Adsorption Ratio (SAR), Sodium Percentage (Na%) and the total hardness (TH) was calculated. The calculation methods can be found in Wang et al. (2024).

3 Results

3.1 Hydrochemical characteristics of river water and groundwater

The physicochemical data of river water and groundwater in the study area is reported in Table 1. The river water exhibits weak alkalinity throughout its entire course, with an average of 8.36. The TDS in the river gradually increases as it flows downstream, with the headwater area recording the lowest TDS at 209 mg/L and the downstream area peaking at 1672 mg/L (Fig. 4). It significantly exceeds the global average TDS for rivers (115 mg/L). Based on the definition of water hardness, the upper reaches of the river (above the Changma Reservoir) fall within the categories of slightly hard ($150 \text{ mg/L} < \text{TH} < 300 \text{ mg/L}$) and hard water ($300 \text{ mg/L} < \text{TH} < 450 \text{ mg/L}$), while the middle reaches (from Changma Reservoir to Shuangta Reservoir) qualify as hard water. The lower reaches of the river (below Shuangta Reservoir) are classified as very hard water ($\text{TH} > 450 \text{ mg/L}$).



Table 1 Basic physical and chemical data for river water and groundwater samples in the Shule River Basin.

No.	Tem (°C)	pH (-)	TDS (mg/L)	Ca ²⁺ (mg/L)	K ⁺ (mg/L)	Mg ²⁺ (mg/L)	Na ⁺ (mg/L)	Cl ⁻ (mg/L)	HCO ₃ ⁻ (mg/L)	SO ₄ ²⁻ (mg/L)	NO ₃ ⁻ (mg/L)	SiO ₂ (mg/L)	δD (‰)	δ ¹⁸ O (‰)	d-excess (‰)
RW01	5.4	8.22	209.00	51.00	1.97	7.70	16.60	12.72	168.73	39.69	1.80	4.67	-58.25	-9.41	17.03
RW02	5.2	8.47	225.00	57.16	1.06	9.95	19.64	14.52	175.38	46.31	3.84	4.54	-59.62	-9.24	14.30
RW03	4.8	8.35	265.00	64.74	1.73	8.47	19.34	26.49	186.40	51.74	3.78	4.33	-60.41	-9.26	13.67
RW04	6.6	8.41	319.00	77.89	1.68	11.86	21.62	31.11	196.73	77.06	3.60	4.12	-58.38	-8.94	13.14
RW05	6.1	8.56	365.00	83.47	1.27	20.45	28.08	38.71	225.20	98.55	3.47	4.29	-61.49	-9.32	13.07
RW06	6.0	8.21	396.00	85.80	1.35	25.90	21.40	47.93	239.88	102.14	4.53	4.37	-62.98	-9.12	9.98
RW07	6.3	8.50	492.00	86.70	1.22	26.30	27.40	51.35	232.05	144.00	5.27	4.63	-60.79	-9.46	14.93
RW08	5.9	8.08	435.00	94.20	1.25	28.80	23.50	49.24	248.41	113.67	4.77	4.50	-61.25	-9.81	17.23
RW09	5.7	8.01	496.00	85.80	1.42	48.50	12.40	64.36	221.64	147.47	5.33	4.92	-78.02	-12.12	18.96
RW10	6.1	8.31	512.00	92.90	1.90	53.30	19.70	65.80	229.00	173.30	2.90	4.11	-60.90	-8.70	8.70
RW11	6.7	8.45	492.00	96.70	2.17	30.40	29.50	41.26	196.75	178.83	5.70	4.79	-58.19	-8.88	12.85
RW12	7.1	8.52	498.60	93.20	2.00	37.50	29.70	70.80	219.20	135.00	2.90	4.24	-61.70	-9.10	11.10
RW13	7.8	8.37	542.60	95.00	2.60	36.40	46.50	61.60	195.60	205.00	1.70	4.56	-53.30	-8.40	13.90
RW14	7.4	8.14	545.10	97.70	3.29	36.20	41.80	65.13	173.83	217.10	6.01	4.71	-52.35	-7.79	9.97
RW15	7.4	8.14	579.00	101.50	3.72	41.50	48.80	72.52	225.21	204.25	4.53	4.54	-55.54	-8.53	12.71
RW16	7.8	8.52	598.00	118.10	3.18	34.50	39.70	67.93	239.93	207.98	4.90	4.50	-49.67	-6.82	4.89
RW17	8.0	8.22	650.20	126.00	3.08	40.30	56.90	84.80	258.69	232.96	3.41	4.63	-50.29	-7.14	6.83
RW18	11.0	8.32	961.00	169.00	2.95	76.80	91.00	155.57	270.86	410.65	1.10	4.33	-60.70	-8.48	7.14
RW19	11.5	8.26	782.40	137.90	2.92	26.80	99.40	160.34	237.16	235.61	0.88	4.58	-52.75	-8.02	11.40
RW20	11.6	8.57	926.40	105.40	4.20	86.20	71.50	136.50	233.60	393.80	1.90	4.90	-52.92	-7.62	8.04
RW21	11.0	8.35	1577.00	163.20	4.10	98.70	175.10	327.40	107.70	708.60	1.60	4.40	-53.04	-7.28	5.20
RW22	11.8	8.44	1410.00	155.70	3.95	98.50	185.60	405.10	244.00	435.30	1.22	4.58	-51.90	-7.62	9.06
RW23	12.4	8.94	1672.00	158.80	5.21	37.30	372.70	631.30	173.00	452.60	1.10	4.92	-32.80	-3.40	-5.60
GW01*	16.9	7.92	704.80	158.95	3.16	30.50	32.62	26.30	310.23	308.90	2.90	4.11	-67.57	-10.08	13.07
GW02*	5.2	7.95	265.00	34.80	2.49	25.01	26.90	22.70	225.77	43.29	0.64	3.92	-84.70	-12.46	14.98
GW03	7.5	7.10	742.00	91.73	4.01	87.35	95.77	60.56	787.16	62.40	0.50	4.15	-79.30	-11.71	14.38
GW04	10.5	7.32	452.00	47.65	3.68	38.39	58.66	54.93	328.49	71.06	1.26	4.13	-62.30	-8.61	6.58
GW05	10.8	7.23	400.00	42.22	3.12	39.18	54.24	63.91	264.08	64.05	1.31	4.00	-64.30	-9.83	14.34
GW06	11.8	8.06	1160.00	94.90	1.80	94.90	166.00	247.13	190.38	508.02	4.69	4.20	-53.73	-7.75	8.29
GW07	12.5	7.79	1382.00	107.50	2.20	122.00	199.00	320.87	161.09	681.05	6.04	4.40	-53.82	-7.95	9.74
GW08	12.20	7.81	967.00	88.30	1.50	62.90	87.90	144.41	214.79	257.46	2.42	3.90	-55.12	-8.27	11.08

'RW' indicate river water samples, while 'GW' stand for groundwater samples. For groundwater samples, an asterisk () represents spring water, while the others are taken from wells.

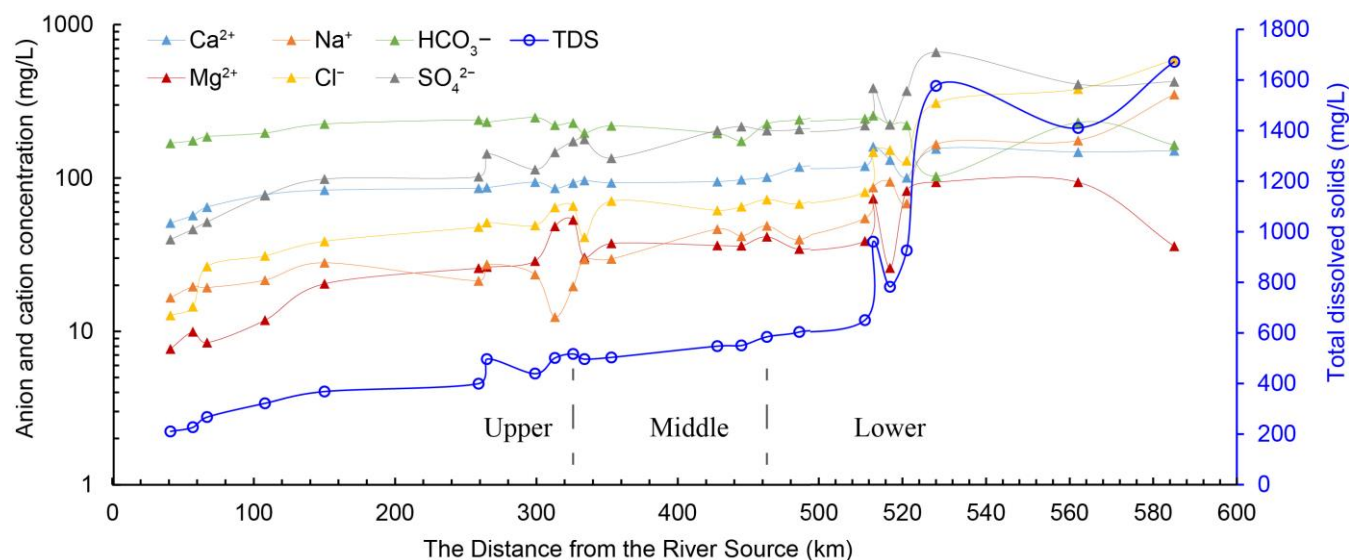


Figure 4: Hydrochemical characteristics changes along Shule River. The x-axis does not use a uniform scale. The left side is the upstream area (samples 1 to 10), the middle is the midstream area (samples 11 to 15), and the right side is the downstream area (samples 16 to 23).

In the upstream river water within the study area, the average mass concentration of major cations follows the order of Ca^{2+} , Mg^{2+} , Na^+ , and K^+ , from highest to lowest. Conversely, in the middle and downstream areas, the average mass concentration of major cations exhibits a different sequence, with Ca^{2+} , Na^+ , Mg^{2+} , and K^+ . Concerning anions, in both the upstream and middle areas, the predominant ion mass concentration is arranged in the order of HCO_3^- , SO_4^{2-} , and Cl^- . However, in the downstream area, the sequence changes to SO_4^{2-} , Cl^- , and HCO_3^- . As a result, the hydrochemical composition of the river water in the upstream area is categorized as Ca^{2+} - HCO_3^- type, while in the middle area, it falls into the Ca^{2+} - Mg^{2+} - HCO_3^- - SO_4^{2-} category. In the downstream region, the river water assumes a Ca^{2+} - Na^+ - SO_4^{2-} - Cl type (Fig. 5).

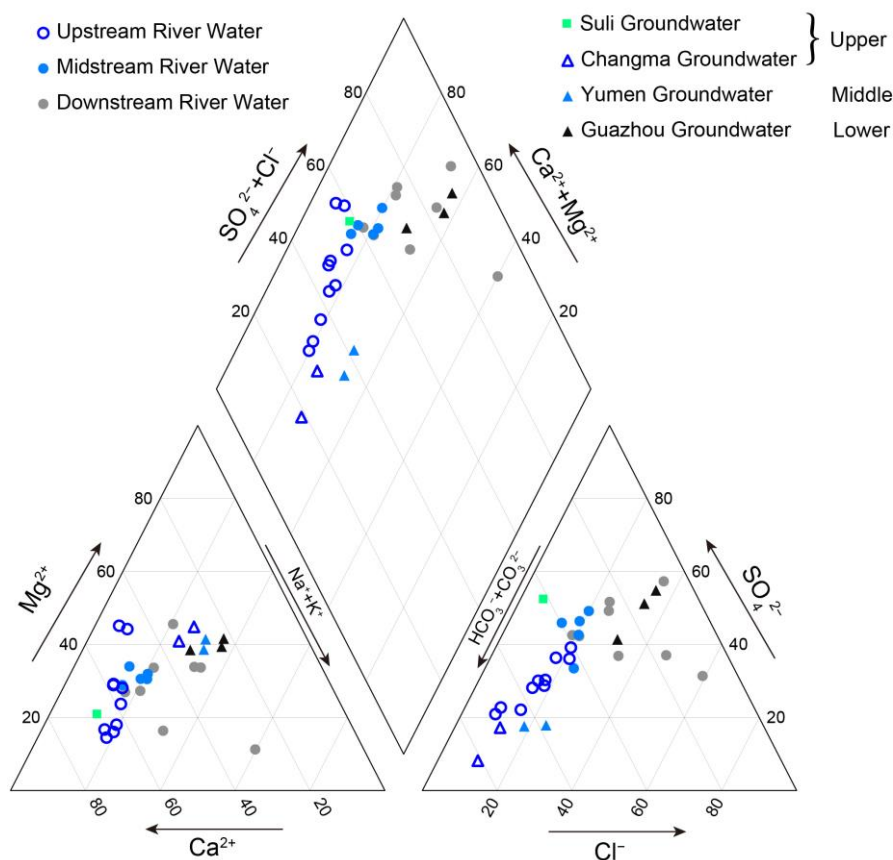


Figure 5: Piper trilinear plots for the chemical compositions of the river water and groundwater in the study area. In order to more clearly understand the changes in the hydrochemical characteristics of groundwater, groundwater samples were classified according to the sampling locations. The upper reaches include Suli and Changma, the middle reaches include Yumen, and the lower reaches include Guazhou.

In the study area, groundwater displays a pH range of 7.1 to 8.06, indicating a weak alkaline nature. The average TDS in groundwater is 759.1 mg/L. Considering the differences in sampling locations, we categorize the groundwater samples into Suli and Changma groundwater from the upstream region, Yumen groundwater from the midstream region, and Guazhou groundwater from the downstream region (Fig. 5). The upstream groundwater samples are collected from the Qilian Mountains, while the midstream and downstream groundwater samples are collected from the Hexi Corridor. Due to the combined effects of climatic conditions and hydrogeological factors, the hydrochemical composition of these groundwater samples exhibits significant variations. Notably, TDS levels are lowest in spring water from the Qilian Mountains region and highest in groundwater from the Guazhou area in the Hexi Corridor. Groundwater chemistry types vary, with the Qilian Mountains region classified as Mg^{2+} - Ca^{2+} - HCO_3^- type, the Yumen Basin as Mg^{2+} - Na^+ - HCO_3^- type, and Guazhou as Mg^{2+} - Na^+ - SO_4^{2-} - Cl^- type.



3.2 Stable Isotopes of River Water and Groundwater

According to the Table 1, in the upper reaches of the Shule River, the $\delta^{18}\text{O}$ values of river water range from -12.12‰ to -8.70‰ , with an average value of -9.54‰ , while the δD values range from -78.02‰ to -58.25‰ , averaging at -62.21‰ (Fig. 6). The d-excess falls within the range of 8.7‰ to 18.96‰ , with an average of 14.10‰ . To the middle reaches of the river, the average $\delta^{18}\text{O}$ and δD values are -8.54‰ and -56.22‰ , respectively, with a d-excess average of 12.11‰ . In the downstream area, the average $\delta^{18}\text{O}$ and δD isotope values in river water are -7.05‰ and -50.51‰ , respectively, and the d-excess averages at 5.87‰ .

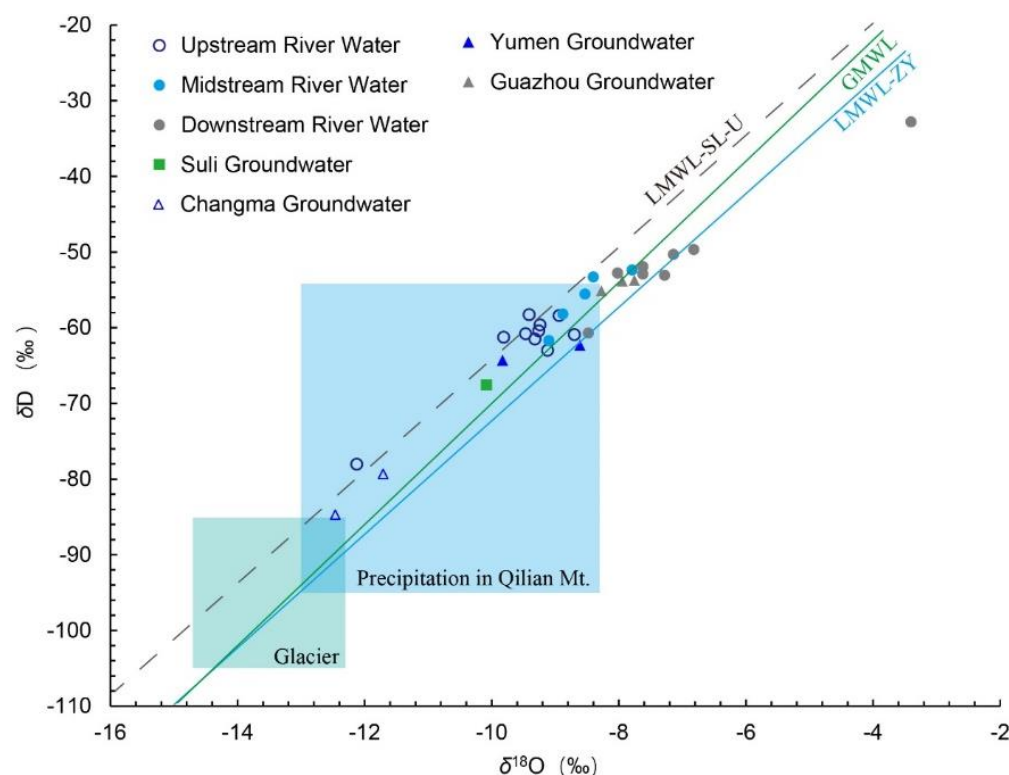


Figure 6 Piper trilinear plots for the chemical compositions of the river water and groundwater in the study area. In order to more clearly understand the changes in the hydrochemical characteristics of groundwater, groundwater samples were classified according to the sampling locations. The upper reaches include Suli and Changma, the middle reaches include Yumen, and the lower reaches include Guazhou.

Concerning groundwater, in the Qilian Mountains region, the $\delta^{18}\text{O}$ values range from -12.46‰ to -10.08‰ , with an average of -11.42‰ , while the δD values range from -84.70‰ to -67.57‰ , averaging at -77.19‰ . The d-excess falls within the range of 8.7‰ to 18.96‰ , with an average of 10.50‰ . In the Yumen area of the Hexi Corridor, the average $\delta^{18}\text{O}$ and δD isotope values of groundwater are -9.22‰ and -63.30‰ , respectively, with a d-excess average of 12.11‰ . Conversely, in the Guazhou area, the average $\delta^{18}\text{O}$ and δD isotope values of groundwater are -7.99‰ and -54.23‰ , respectively, with a d-excess average of 9.7‰ .



4 Discussion

4.1 Isotopic Characteristics of River Water

245 Precipitation serves as not only a crucial element within the hydrological cycle but also as the primary recharge source for rivers and groundwater (Galewsky et al., 2016; Wang et al., 2022). It is commonplace to juxtapose the $\delta^{18}\text{O}$ and δD values of river water and groundwater with precipitation in studying the hydrological cycle to analyze their interconnectedness (Wang et al., 2023). Given the significant climatic and geographical differences between the Qilian Mountains and the Hexi Corridor, the isotopic characteristics in precipitation also vary. Therefore, it is necessary to establish local meteoric water lines (LMWL) based on linear regression of δD and $\delta^{18}\text{O}$ values in precipitation for each region. Therefore, LMWLs were established for the high-altitude Qilian Mountains region in the upper reaches of the Shule River (LMWL-SL-U: $\delta\text{D} = 7.4 \times \delta^{18}\text{O} + 9.86$, Guo et al., 2022) and the low-altitude Hexi Corridor plain in the middle and lower reaches (LMWL-ZY: $\delta\text{D} = 7.5 \times \delta^{18}\text{O} + 2.7$, IAEA and WMO, 2006), respectively. The LMWL-SL-U was obtained using the data provided by Guo et al. (2022). For the LMWL-ZY, data from a long-term monitoring station located 350 kilometers east of the study area, was established by the IAEA (Wang et al., 2015).

The isotopic analysis results were graphed with the GMWL and the LMWL in Fig. 6. Most river water samples fall along with the LMWL-SL-U, suggesting that the meteoric water is the major sources to the river water. Interestingly, the downstream river water isotopes fall apart from the LMWL-SL-U into the LMWL-ZY and these isotopic values are more positive. Theoretically, the δD and $\delta^{18}\text{O}$ values in river water in the upstream area of the study region would purely reflect the isotopic characteristics of precipitation in the Qilian Mountains. In contrast, in the downstream areas, these would manifest as a mixture of precipitation from the Qilian Mountains and the Hexi Corridor plains. This explains why the isotopic scatter plot of river water gradually shifts from the LMWL-SL-U to the LMWL-ZY. Additionally, Fig. 6 illustrates that the isotopic composition of river water in the study area exhibits a progressively positive trend from upstream to downstream. This trend is likely due to evaporation effects experienced by the river water after a prolonged runoff process. Kalvāns et al. (2020) found that evaporation of water impounded on the soil surface is an important mechanism leading to isotopic enrichment of surface water. Considering the scarce rainfall in the Hexi Corridor region and the relatively weak contribution of precipitation to river runoff, we believe the strong evaporation in the study area, whether occurring in the river water or in the soil water, is the main factor affecting the isotopic changes in the river water along the runoff process. In other words, due to the intense evaporation in the SRB, the isotopic values of river water become increasingly positive as it flows from the upstream to the downstream, progressively diverging from the LMWL-SL-U.

Using the linear regression method, we found that the $\delta^{18}\text{O}$ -altitude gradient for the Shule River water is approximately $-0.08\text{‰}/100\text{m}$, suggesting that the $\delta^{18}\text{O}$ values in river water will decrease with increasing elevation. In comparison, in the Heihe River basin, which is located about 300km southeast of the study area, the altitudinal isotopic gradient of precipitation is $-0.18\text{‰}/100\text{m}$ (Wang et al., 2009). Similarly, the altitudinal isotopic gradient of precipitation and river water ranges from



275 $-0.1\%/100\text{m}$ to $-0.3\%/100\text{m}$ in the Qinghai-Tibet Plateau region (Li and Garzzone, 2017). It is evident that the pattern of isotopic variations in river water with elevation within the study area closely resembles that observed in adjacent regions. By comparing the isotopic characteristics of river water with those of precipitation, it becomes evident that the isotopic points of river water in the Shule River's upper and middle reaches largely fall into the isotopic range of precipitation in the Qilian Mountains (Fig. 5). Furthermore, the data points for isotopes in the river water in the middle and lower reaches fall to the left of the LMWL-ZY, indicating that precipitation in the Hexi Corridor plain is not the primary source for the river in the middle and lower reaches. Therefore, it can be inferred that the runoff in the Shule River is primarily sourced from the Qilian Mountains in the upper reaches, which aligns with previous research findings (Wu et al., 2021; Zhou et al., 2021). This is a typical phenomenon in arid regions: water resources, whether from rivers or groundwater (Wang et al., 2015), are primarily generated in mountainous areas due to abundant precipitation and snowmelt. In contrast, precipitation in plains is often insufficient to replenish rivers or groundwater to a level that makes them a significant resource for human use.

4.2 Factors controlling river water hydrochemistry

The sources of major ions in the river water include atmospheric transport of sea salt components, weathering products of soluble rocks (comprising evaporites, silicates, carbonates, and sulfides), and pollutants generated by human activities. In the upper reaches of the Shule River, human presence is scarce, while human activities are more frequent in the middle and lower reaches. Consequently, the major ions in the river water may be influenced by both natural processes and human activities. The Gibbs diagrams and ion correlation analysis results can provide a foundational understanding of the sources of ionic components in river water.

4.2.1 Gibbs diagram

The potential sources of dissolved ions in river water encompass marine salts carried by atmospheric precipitation, soluble rock weathering products, and pollutants generated by human activities (Hu et al., 1982; Raymond et al., 2008). In comparison to tropical monsoon regions, the study area experiences lower precipitation levels, resulting in a relatively minor impact of solutes carried by rainfall on the ionic composition of river water. The weathering of carbonate rocks, silicate rocks, and evaporites in the study area constitutes the primary potential sources of ions in river water. The Gibbs diagram has been widely utilized for interpreting the origins of river water's hydrochemical characteristics and stands as a crucial tool for qualitatively determining the sources of ions in river water (Gibbs, 1970; Marandi and Shand, 2018).

The Gibbs diagram depicted in Fig. 7 is constructed based on the correlation between the primary ion ratios and TDS in the Shule River water. All river water samples fall within the Gibbs model, indicating that the solutes in the Shule River water are largely impacted by rock weathering and evaporation. Furthermore, the TDS values of river water mainly range from 100 to 1000 mg/L, and the mean $\text{Na}^+(\text{Na}^+ + \text{Ca}^{2+})$ ratio is 0.19 in the upstream river water, 0.26 in the middle stream river water, and 0.41 in the downstream river water. Additionally, the mean $\text{Cl}^-(\text{Cl}^- + \text{HCO}_3^-)$ ratio is 0.23 in the upstream river water, 0.34 in



the middle stream river water, and 0.58 in the downstream river water, indicating that the ion sources in these areas align with the Rock Weathering Type. This observation is consistent with the findings reported by Zhou et al. (2014).

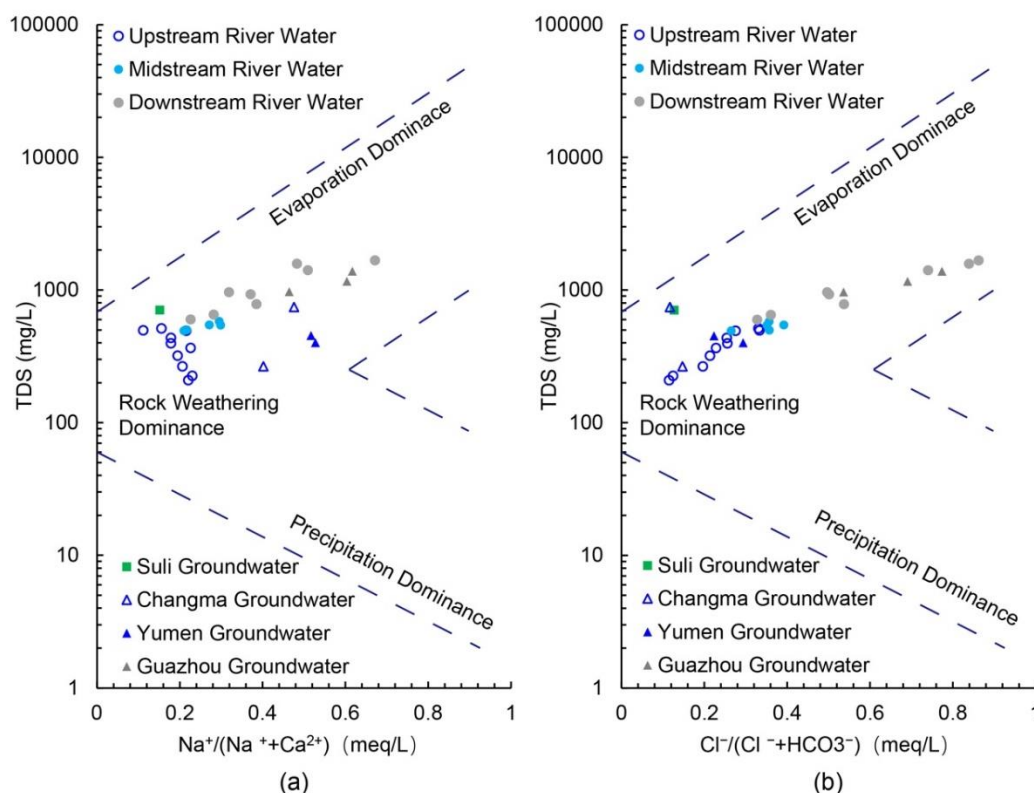


Figure 7 Gibbs diagrams generated based on Shule River water data and groundwater data, (a) TDS versus Na^+ , (b) TDS versus Cl^- .

4.2.2 Ion ratios

The Gibbs model has preliminarily reveal the source of major ions in Shule River water. To clarify further into understanding the potential impact of various mineral weathering processes on river water ions within the study area, a sodium-normalized mixing diagram was made in Fig. 8. The results reveal that river water samples predominantly cluster between silicate and carbonate rocks, with a closer alignment to silicate rock types. This suggests that the ions in river water primarily originate from the weathering of silicate rocks, but the contribution from the weathering products of carbonate rocks should not be underestimated. It's noteworthy that the Ca^{2+}/Na^+ , Mg^{2+}/Na^+ , and HCO_3^-/Na^+ ratios in the upstream river water of the study area exceed those in the middle and downstream river water. This signifies that carbonate rock weathering in the upstream region exerts a more pronounced impact on the major ions in the river water. This phenomenon is not only linked to the extensive exposure of carbonate rock formations in the upstream region but also to the fact that, under similar natural conditions, carbonates exhibit significantly higher solubilities (12–40 times) than silicates, making them more susceptible to weathering (Meybeck, 1987).

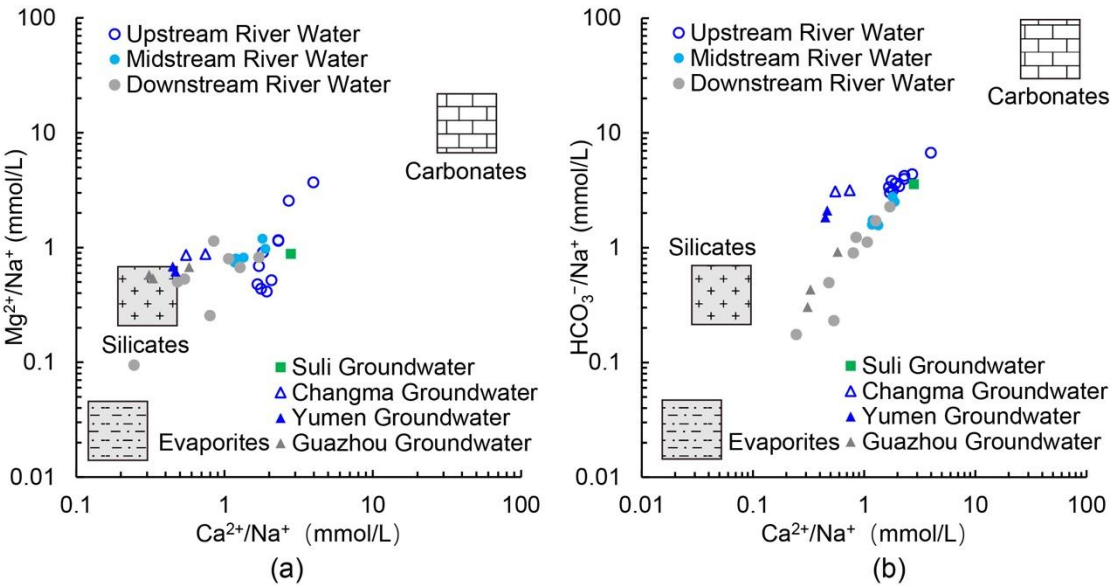


Figure 8 Mixing diagram of the Na-normalized molar ratios of (a) Ca^{2+} versus Mg^{2+} and (b) Ca^{2+} versus HCO_3^- in the Shule river. The data for the three endmembers, i.e., carbonates, silicates and evaporites, are obtained from Gaillardet et al. (1999).

4.2.3 Correlation of various ions

The processes of mineral weathering and dissolution, as well as the evaporation concentration of river water, play a role in dictating the ionic composition of river water. In-depth analysis can further understand the causes of river water hydrochemistry and the control mechanisms of its evolution. The above process engender linear relationships among specific ions, thereby warranting an examination of the linear correlation coefficients between distinct ionic species as a diagnostic tool for discerning the origins of these ions in river water. Generally, when ions exhibit a robust positive linear correlation, it implies a common mass source or involvement in concurrent chemical reactions. We have calculated the correlation coefficients among ions in the Shule River water and presented them in Table 2. Values closer to 1 in this table indicate a stronger positive correlation between the respective ion pairs.

Table 2 Correlation matrix of hydrochemical compositions in Shule River water

	pH	TDS	Ca^{2+}	K^+	Mg^{2+}	Na^+	Cl^-	HCO_3^-	SO_4^{2-}	NO_3^-	SiO_2
pH	1										
TDS	0.415*	1									
Ca^{2+}	0.240	0.892**	1								
K^+	0.355	0.837**	0.751**	1							
Mg^{2+}	0.053	0.758**	0.731**	0.621**	1						
Na^+	0.570**	0.907**	0.745**	0.780**	0.439*	1					
Cl^-	0.530**	0.935**	0.765**	0.767**	0.531**	0.987**	1				

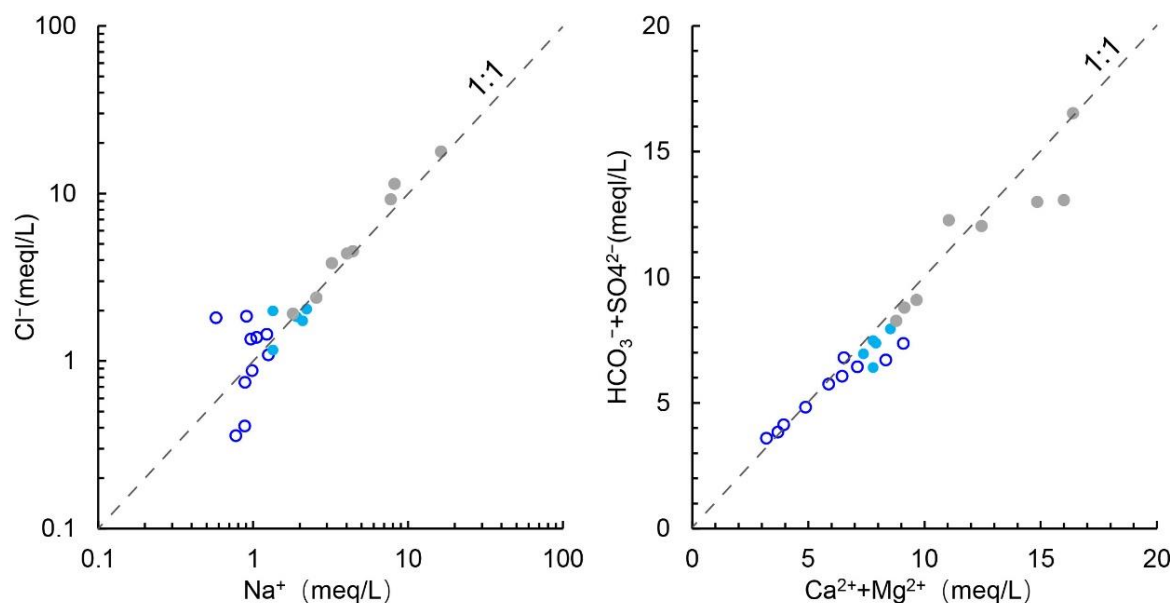


HCO ₃ ⁻	-0.170	-0.169	0.126	-0.162	0.074	-0.248	-0.208	1			
SO ₄ ²⁻	0.276	0.942**	0.878**	0.809**	0.859**	0.741**	0.770**	-0.214	1		
NO ₃ ⁻	-0.354	-0.578**	-0.523*	-0.490*	-0.423*	-0.575**	-0.571**	0.071	-0.532**	1	
SiO ₂	0.072	0.282	0.127	0.395	0.129	0.329	0.309	-0.090	0.215	0.079	1

Significant value (** p <0.01, * p <0.05)

It is evident that the correlation coefficients between Ca²⁺, K⁺, Na⁺, Cl⁻, SO₄²⁻ and TDS in the river water are highly significant, all exceeding 0.8. This suggests their substantial contribution to the salinity of the river water. Furthermore, the correlation coefficients between Ca²⁺, Mg²⁺ and SO₄²⁻ surpass 0.85, which indicates that these three ions may originate from the dissolution of CaSO₄ and MgSO₄. Notably, the correlation coefficient between Na⁺ and Cl⁻ is 0.987, very close to 1, and their respective correlation coefficients with TDS are also greater than 0.9. This implies that Na⁺ and Cl⁻ share a common source and make a pronounced contribution to the salinity of the river water. It is likely that the Na⁺ and Cl⁻ sources may mainly be the inputs of the sea salt brought by the atmospheric circulation and the salt particles of the air in the study area. Similar findings have been reported in the SRB, eastern of the Hexi Corridor (Zhang et al., 2021). In addition, the correlation coefficients between NO₃⁻ and the other ions are all less than 0.4, indicating a potentially closer association with human activities rather than natural process (Huang et al., 2014).

To gain insight into the interrelationships among ions in Shule River water, Na⁺ versus Cl⁻ and (Ca²⁺ Mg²⁺) versus (HCO₃⁻ + SO₄²⁻) diagrams were created and presented in Fig. 9. It can be seen that the Na⁺/Cl⁻ points in upstream river water deviates from the 1:1 line, while points for downstream river water samples closely align with the 1:1 line. Factors affecting Na⁺ in water and their ratio to Cl⁻ include evaporite dissolution, ion-exchange adsorption, and human activities. Whereas human activities are very rare in the very upstream area of the Shule River, we consider that in the very upstream region, the dissolution of silicates predominantly influences the source of Na, while downstream, the dissolution of salt rocks becomes the dominant factor. As a result, the Na⁺ versus Cl⁻ ratios show a clear difference between upstream and downstream (Fig. 9a). The average Na⁺/Cl⁻ ratio in river water is 1.16, which is similar to the world average ratio in seawater (1.15). This shows that the sea salt carried by the atmospheric circulation has a certain influence on the ion composition of Shule River water. Furthermore, the concentration of Na⁺ exceeded the concentration Cl⁻, which also may indicate that halite dissolution was not the only source for Na⁺. For example, in the case of groundwater recharging a river, the concentration of Na⁺ in the water will increase after cation exchange occurs after the pore water flows through the formation. Moreover, silicate weathering could release Na⁺ into the river water (Guo et al., 2015). In addition, a linear relationship is found between (Ca²⁺ Mg²⁺) and (HCO₃⁻ + SO₄²⁻), with their ratios clustering in the range of 0.88 to 1.24, and an average value of 1.06. If the ratio of (Ca²⁺ Mg²⁺) and (HCO₃⁻ + SO₄²⁻) is strictly 1:1, then it can be assumed that these four ions in river water are controlled by the dissolution of carbonate rocks. However, it is clear that some points deviate from the 1:1 line as shown in Fig 9b. Thus, in addition to carbonate rocks dissolution, silicate weathering plays a role in influencing the levels of these four ions in river water, as previously mentioned.



365 **Figure 9** Piper trilinear plots for the chemical compositions of the river water and groundwater in the study area. In order to more clearly understand the changes in the hydrochemical characteristics of groundwater, groundwater samples were classified according to the sampling locations. The upper reaches include Suli and Changma, the middle reaches include Yumen, and the lower reaches include Guazhou.

4.3 The Groundwater Recharge Sources and Evolutionary Processes

370 As the SRB is situated in an arid region with scarce rainfall, its water resources predominantly comprise river water and groundwater. Groundwater is known for its slow flow and comparatively stable properties in the aquifer. In light of the limited number of groundwater samples collected in this study, our discussion relies on the outcomes of our sample analysis, complemented by existing research in the field of groundwater, to provide a comprehensive understanding of the regional hydrological cycle.

375 4.3.1 Groundwater Recharge Sources

The groundwater within the SRB was broadly divided into segments corresponding to the upper, middle, and lower reaches of the river: Suli groundwater and Changma groundwater (upper reaches), Yumen groundwater (middle reaches), and Guazhou groundwater (lower reaches). A comparative analysis was conducted to investigate the isotopic characteristics of groundwater and river water in these regions (Fig. 6). In the upper reaches of the SRB, which include areas such as the headwater region, Changma alluvial fan, and Yumen alluvial fan, the points of $\delta^{18}\text{O}$ and δD in groundwater are distributed closely along the LMWL-SL-U (Fig. 6). This alignment indicates a strong interconnection between river water and groundwater in this region. Moreover, the $\delta^{18}\text{O}$ and δD values of groundwater in the upper reaches largely fall within the isotopic rectangular range characterizing Qilian Mountains' precipitation (Fig. 6). They exhibit a slight deviation from the glacial end-member but



manifest a more negative offset compared to river water isotopes. This suggests that in addition to precipitation, glacial meltwater constitutes another important source of recharge to the river. Using isotopic data, Zhou et al. (2015) estimated the contribution of groundwater, precipitation and glaciers to the Shule river water to be 67%, 20% and 13% in the headwater region, respectively. Despite some uncertainties, it is still clear that in the upper reaches of the Shule River, the river is recharged by a combination of groundwater, precipitation and glacial water.

In the middle reaches of the SRB (near Yumen City), the distribution range of isotopic values of groundwater mostly overlaps with that of upstream river water. This indicates that there is a close hydraulic connection between them. Wang et al. (2015) also pointed out that in the middle reaches of the Shule River, the recharge effect of local atmospheric precipitation on groundwater is very weak or even negligible. Guo et al. (2015) concluded that the contribution of local atmospheric precipitation to groundwater is only 1%.

As we move downstream along the Shule River, the $\delta^{18}\text{O}$ and δD composition of groundwater gradually diverges from the LMWL-SL-U. However, a significant portion still resides on the left side of the LMWL-ZY. In the downstream region, the isotope composition of groundwater exhibits substantial overlap with surface water, indicating a robust hydraulic linkage between the two. Considering the hydrogeological conditions and river characteristics here, and combining the previous research findings of Wang et al. (2016) who used hydrochemical evolution to study the groundwater in Guazhou, it can be reasonably concluded that groundwater in the downstream region is primarily recharged by Shule River water, with contributions from local precipitation in the Hexi Corridor recharge being negligible.

4.3.2 The Hydrochemical Evolution of Groundwater

The hydrochemical characteristics of groundwater in the study area are influenced not only by their recharge sources but, to a larger extent, by the interactions between groundwater and the aquifer during the groundwater flow. Combining the data from this study with previous research findings (Wang et al., 2015, 2016, Guo et al., 2015), it is evident that the groundwater recharge in the study area originates from the Qilian Mountains region. Vadose zone in this region comprises gravel with relatively large pore spaces, allowing both precipitation and river water to easily infiltrate and form groundwater. Subsequently, under the control of the topography, lateral flow recharges the Yumen alluvial fan, continuing downstream. Therefore, in the upper and middle reaches, after low salinity precipitation and river water transform into groundwater, the minerals in the aquifer readily react with them. The hydrochemical processes in groundwater are predominantly governed by dissolution of halite, calcite, dolomite and gypsum in these areas.

4.4 Water quality for drinking and irrigation

The SRB, characterized by a significantly higher annual evaporation rate compared to precipitation, stands as one of the most arid regions in China. Nevertheless, this area accommodates an extensive irrigation network spanning over 1.3 million acres, providing a robust foundation for local socioeconomic development and human livelihood (Ma et al., 2018). Consequently, the water quality of both surface water and groundwater in the SRB directly impacts regional ecological security and



sustainable socioeconomic progress. In this context, we evaluate the suitability of river water and groundwater for drinking and irrigation based on parameters such as TH, $\text{Na}^+\%$, SAR, and NO_3^- concentration.

In the Shule River's headwaters region, 50% of the water samples are classified as slightly hard, and the remaining 50% are categorized as hard water. As we move to the middle reaches, the water is consistently characterized as hard, and in the downstream areas, it becomes very hard, demonstrating a gradual deterioration in water quality from upstream to downstream. A similar pattern is observed in the groundwater quality within the study area. However, it's worth noting that in the arid SRB, the water quality remains relatively acceptable despite this progression towards harder water.

In the upper reaches of the Shule River, the $\text{Na}^+\%$ value in river water ranges from 6.05 to 18.69, with an average value of 14.25. This range categorizes the water as excellent, making it suitable for irrigation. In the middle reaches, among the five samples, only one exceeds a $\text{Na}^+\%$ value of 20 (20.48), while the remaining samples also qualify as excellent for irrigation. Downstream, the $\text{Na}^+\%$ value in river water samples varies from 16.3 to 59.17, with an average of 29.18. Of the eight samples in the downstream area, 25% are considered excellent, 12.5% fall into the permissible range, and the rest maintain a good quality rating. Conversely, all groundwater samples meet the criteria for excellent quality according to the $\text{Na}^+\%$ value. This implies that both river water and groundwater in the SRB are well-suited for irrigation purposes.

The concentration of nitrates in water often serves as a pivotal indicator for assessing the potential influence of human activities on aquatic ecosystems. This is particularly relevant due to the nitrate emissions associated with agricultural practices and livestock husbandry. In the study area, the nitrate concentration exhibited a range from 0.88 mg/L to 6.01 mg/L, with a mean concentration of 3.32 mg/L. Notably, the nitrate levels in the waters of the Shule River consistently remained below the stipulated standards set by the World Health Organization for nitrate levels in potable water, which is 10 mg/L.

4.5 Implications for the regional hydrological cycle processes

The SRB, situated in the arid northwest region of China, stands out due to its limited precipitation and heightened evaporation. By combining the fundamental hydrological cycle elements with the isotopic characteristics of various water sources, such as precipitation (Zhou et al. 2015, 2022; IAEA and WMO, 2003), glacial meltwater (Zhou et al., 2015), river water, and groundwater, the hydrological cycle processes in the study area can be clearly elucidated. Existing research results indicate that the upper reaches of the Shule River serve as the genesis of regional water resources, where precipitation and glacial meltwater readily recharge both river water and groundwater, establishing a vital water supply area for the region (Guo et al., 2015; He et al., 2015; Wang et al., 2016; Wang et al., 2017; Wang et al., 2015; Xie et al., 2022). In contrast, the middle and lower reaches struggle to receive effective recharge from scarce precipitation into groundwater (Fig. 10). However, a discernible hydraulic connection exists between river water and groundwater in these regions. From a hydrogeological perspective, in the vicinity of the Yumen alluvial fan, numerous springs overflow, ultimately feeding into the river again, constituting a zone where groundwater recharges surface water (Fig. 3). Further downstream, in the Guazhou area, river water is extensively employed for agricultural irrigation and subsequently infiltrates, recharging groundwater. Consequently, in the



middle and lower reaches of the SRB, there is a close relationship between groundwater and surface water, marked by frequent exchanges (Fig. 10).

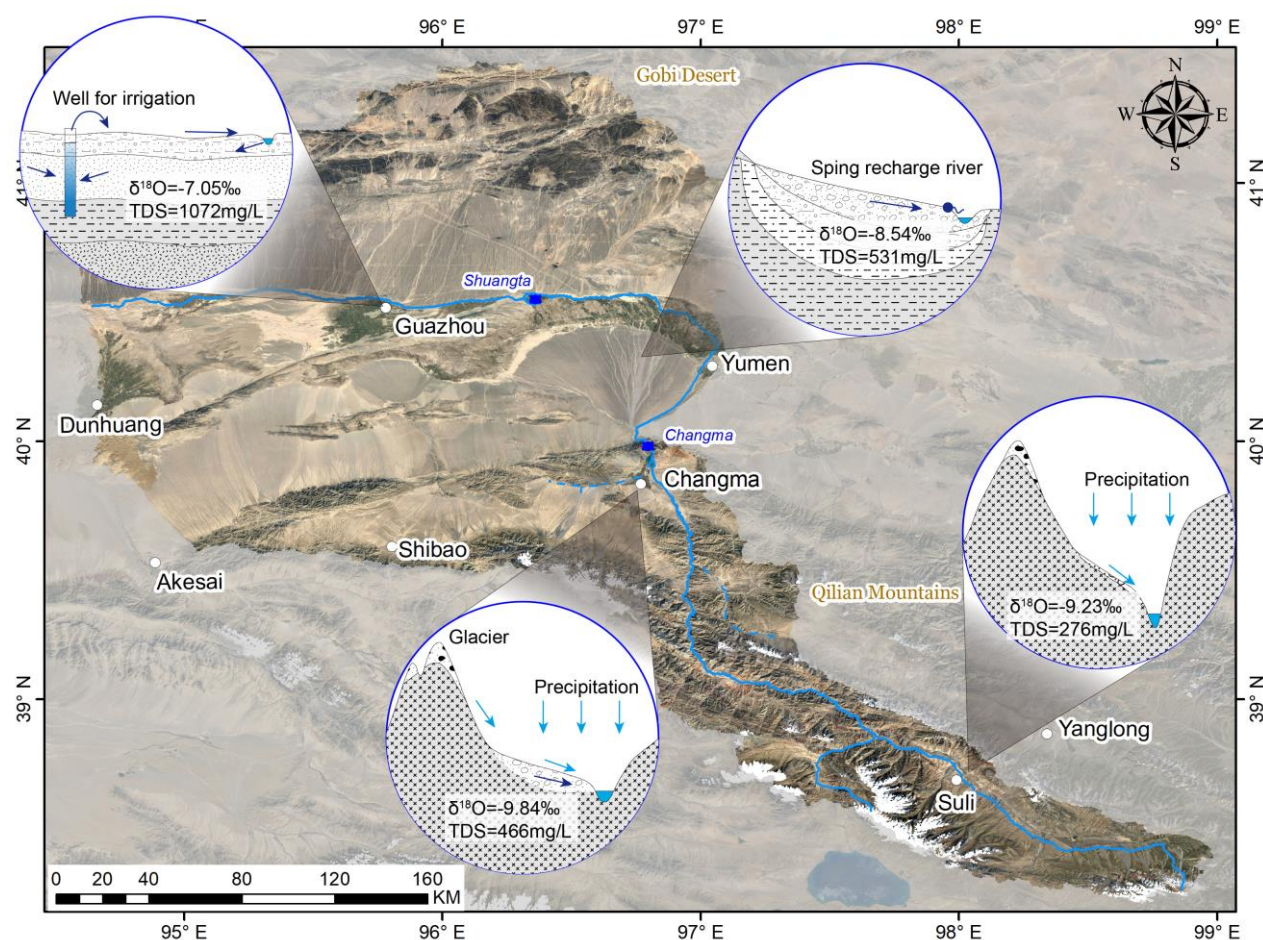


Figure 10 Conceptual model of the hydrological cycle and water quality overview of the Shule River Basin. The base map is derived from satellite imagery of the study area (Source: © Google Earth, accessed January 2025, Google Inc.).

Furthermore, combined with the hydrochemical features of river water and groundwater, the factors influencing regional water resource quality can be illustrated. The chemical composition of water in the Shule River is influenced by processes such as rock chemical weathering, including silicates and carbonates. Furthermore, evaporation also plays a non-negligible role in the hydrochemical features of river water. The chemical makeup of groundwater, on the other hand, is primarily controlled by water-rock interactions, involving mechanisms such as mineral dissolution and ion exchange. Both river water and groundwater are suitable for agricultural irrigation; however, in terms of drinking water quality, they are considered to be slightly hard. This not only establishes a scientific foundation for the prudent allocation and sustainable development of local water resources but also serves as a basis for the effective management of water resources and the enhancement of drinking water quality.



5. Conclusions

As a crucial agricultural and oasis area, and a typical river-groundwater system, in the arid inland of Central Asia China, the SRB faces the challenge of water scarcity. Therefore, this study utilizes the isotopic and hydrochemical tools to analyze the relationship between river water and groundwater, providing a scientific foundation for the sustainable development and utilization of regional water resources.

The $\delta^{18}\text{O}$ value in Shule River water exhibit an altitude effect, with a gradient value of $-0.08/100\text{m}$, which is lower than that observed in the Qinghai-Tibet Plateau and Hexi Corridor region. Furthermore, in the upper reaches of the Shule River, both river water and groundwater isotopic data points align along the atmospheric line of the Qilian Mountains, matching the isotopic distribution of precipitation, while isotopic values of groundwater are generally more negative than that of river water. This indicates that groundwater is one of the important sources of recharge for the river. In the middle and lower reaches, both water types gradually deviate from the LMWL due to evaporation, becoming enriched in isotopes. Their isotopic distributions overlap, especially in the lower reaches, and when combined with local agricultural irrigation, it can be concluded that river has become an important source of groundwater. Chemical weathering processes of silicate and carbonate minerals significantly influence the chemical composition of river water, while dissolution and ion exchange reactions play crucial roles in shaping the hydrochemical composition of groundwater. From parameters such as hardness, sodium adsorption ratio, sodium excess, and nitrate concentration, it is evident that both river water and groundwater in the study area are highly suitable for agricultural irrigation, but they are slightly hard for drinking purposes.

Understanding the exchange processes among different water sources in arid regions is essential for the rational allocation and sustainable development of water resources. However, the pronounced isotopic fractionation caused by intense evaporation makes it challenging to quantitatively track the transition of different water sources. Therefore, the next focus of our research will be on quantitative investigations utilizing more stable tracers that are less influenced by environmental and biogeochemical processes.

Data availability

All data is available in Table 1. Map data can be downloaded from the United States Geological Survey.

Author contribution

Conceptualization: LW and YD; Funding acquisition: YD; Investigation: LW and YS; Resources: CY; Visualization: LW and CY; Writing – original draft: LW and CY, Writing -review and editing: YD.



Competing interests

490 The authors declare that they have no conflict of interest.

Financial support

This research has been supported by the Second Tibetan Plateau Scientific Expedition and Research Program (STEP) (Grant No. 2019QZKK0904).

References

- 495 Aravena, R., Herrera, C., Urrutia, J., Hydrochemical and isotopic evaluation of groundwater and river water in the transboundary Silala River watershed. *WIREs Water*, n/a(n/a): e1679. DOI:https://doi.org/10.1002/wat2.1679
- Banerjee, D., Ganguly, S., 2023. A Review on the Research Advances in Groundwater–Surface Water Interaction with an Overview of the Phenomenon. *Water*, 15(8): 1552.
- Bershaw, J., Penny, S.M., Garzione, C.N., 2012. Stable isotopes of modern water across the Himalaya and eastern Tibetan Plateau: Implications for estimates of paleoelevation and paleoclimate. *Journal of Geophysical Research: Atmospheres* (1984–2012), 117(D2). DOI:10.1029/2011jd016132
- 500 Cai, Y., You, C.-F., Wu, S.-F., Cai, W.-J., Guo, L., 2020. Seasonal variations in strontium and carbon isotope systematics in the Lower Mississippi River: Implications for chemical weathering. *Chem. Geol.*, 553: 119810. DOI:https://doi.org/10.1016/j.chemgeo.2020.119810
- 505 Cocca, D. et al., 2023. Assessment of the groundwater recharge processes of a shallow and deep aquifer system (Maggiore Valley, Northwest Italy): a hydrogeochemical and isotopic approach. *Hydrogeology Journal*. DOI:10.1007/s10040-023-02727-1
- Craig, H., 1961. Isotopic Variations in Meteoric Waters *Science*, 133(3465): 1702-1703. DOI:10.1126/science.133.3465.1702
- Crosbie, R., Wang, B., Kim, S., Mateo, C., Vaze, J., 2023. Changes in the surface water – Groundwater interactions of the Murray-Darling basin (Australia) over the past half a century. *J. Hydrol.*, 622: 129683. DOI:https://doi.org/10.1016/j.jhydrol.2023.129683
- 510 da Cunha, A.C., Sternberg, L.d.S.L., 2018. Using stable isotopes ^{18}O and ^2H of lake water and biogeochemical analysis to identify factors affecting water quality in four estuarine Amazonian shallow lakes. *Hydrol. Processes*, 32(9): 1188-1201. DOI:https://doi.org/10.1002/hyp.11462
- 515 Dansgaard, W., 1964. Stable isotopes in precipitation. *Tellus*, 16(4): 436-468. DOI:10.1111/j.2153-3490.1964.tb00181.x
- Fang, X. et al., 2005. Magnetostratigraphy of the late Cenozoic Laojunmiao anticline in the northern Qilian Mountains and its implications for the northern Tibetan Plateau uplift. *SCIENCE IN CHINA SERIES D EARTH SCIENCES-ENGLISH EDITION*-, 48(7): 1040.



- Gaillardet, J., Dupré, B., Louvat, P., Allègre, C.J., 1999. Global silicate weathering and CO₂ consumption rates deduced from the chemistry of large rivers. *Chem. Geol.*, 159(1): 3-30. DOI:https://doi.org/10.1016/S0009-2541(99)00031-5
- Galewsky, J. et al., 2016. Stable isotopes in atmospheric water vapor and applications to the hydrologic cycle. *Rev. Geophys.*, 54(4): 809-865. DOI:https://doi.org/10.1002/2015RG000512
- Gibbs, R.J., 1970. Mechanisms Controlling World Water Chemistry. *Science*, 170(3962): 1088-1090. DOI:doi:10.1126/science.170.3962.1088
- Glok-Galli, M. et al., 2022. Application of hydrochemical and multi-isotopic (⁸⁷Sr/⁸⁶Sr, $\delta^{13}\text{C}$ -DIC, $\delta^2\text{H}$ -H₂O, $\delta^{18}\text{O}$ -H₂O) tools to determine contamination sources and processes in the Guadalhorce River Basin, southern Spain. *Sci. Total Environ.*, 828: 154424. DOI:https://doi.org/10.1016/j.scitotenv.2022.154424
- Guidah Chabi, B. et al., 2023. Characterising groundwater and surface-water interconnections using hydrogeology, hydrochemistry and stable isotopes in the Ouémé Delta, southern Benin. *Hydrogeology Journal*, 31(5): 1229-1243. DOI:10.1007/s10040-023-02645-2
- Guo, J. et al., 2023. Assessment and Identification of Primary Factors Controlling Yangtze River Water Quality. *ACS ES&T Water*, 3(5): 1329-1340. DOI:10.1021/acsestwater.2c00645
- Guo, X. et al., 2015. Stable isotopic and geochemical identification of groundwater evolution and recharge sources in the arid Shule River Basin of Northwestern China. *Hydrol. Processes*, 29(22): 4703-4718. DOI:10.1002/hyp.10495
- Hamidi, M.D., Gröcke, D.R., Kumar Joshi, S., Christopher Greenwell, H., 2023. Investigating groundwater recharge using hydrogen and oxygen stable isotopes in Kabul city, a semi-arid region. *J. Hydrol.*, 626: 130187. DOI:https://doi.org/10.1016/j.jhydrol.2023.130187
- He, J., Ma, J., Zhao, W., Sun, S., 2015. Groundwater evolution and recharge determination of the Quaternary aquifer in the Shule River basin, Northwest China. *Hydrogeology journal*, 23(8): 1745.
- Herath, I.K., Wu, S.J., Ma, M.H., Jianli, W., Chandrajith, R., 2019. Tracing controlling factors of riverine chemistry in a headwater tributary of the Yangtze River, China, inferred from geochemical and stable isotopic signatures. *Environ. Sci. Pollut. Res.*, 26(23): 23899-23922. DOI:10.1007/s11356-019-05598-w
- Herczeg, A.L., Leaney, F., 2011. Environmental tracers in arid-zone hydrology. *Hydrogeology Journal*, 19(1): 17.
- Herrera, C. et al., 2023. Evaluation of the impact of the intensive exploitation of groundwater and the mega-drought based on the hydrochemical and isotopic composition of the waters of the Chacabuco-Polpaico basin in central Chile. *Sci. Total Environ.*, 895: 165055. DOI:https://doi.org/10.1016/j.scitotenv.2023.165055
- Hu, M.-h., Stallard, R.F., Edmond, J.M., 1982. Major ion chemistry of some large Chinese rivers. *Nature*, 298(5874): 550-553. DOI:10.1038/298550a0
- Huang, J., Huang, Y., Zhang, Z., 2014. Coupled Effects of Natural and Anthropogenic Controls on Seasonal and Spatial Variations of River Water Quality during Baseflow in a Coastal Watershed of Southeast China. *PLoS One*, 9(3): e91528. DOI:10.1371/journal.pone.0091528



- Jafari, T., Kiem, A.S., Javadi, S., Nakamura, T., Nishida, K., 2021. Using insights from water isotopes to improve simulation of surface water-groundwater interactions. *Sci. Total Environ.*, 798: 149253. DOI:<https://doi.org/10.1016/j.scitotenv.2021.149253>
- 555 Jasechko, S., Perrone, D., 2021. Global groundwater wells at risk of running dry. *Science*, 372(6540): 418-421. DOI:[doi:10.1126/science.abc2755](https://doi.org/10.1126/science.abc2755)
- Kalvāns, A., Dēliņa, A., Babre, A., Popovs, K., 2020. An insight into water stable isotope signatures in temperate catchment. *J. Hydrol.*, 582: 124442. DOI: <https://doi.org/10.1016/j.jhydrol.2019.124442>
- Kim, M.-S. et al., 2023. Innovative approach to reveal source contribution of dissolved organic matter in a complex river watershed using end-member mixing analysis based on spectroscopic proxies and multi-isotopes. *Water Res.*, 230: 119470. DOI:<https://doi.org/10.1016/j.watres.2022.119470>
- 560 Kuang, X. et al., 2019. Using stable isotopes of surface water and groundwater to quantify moisture sources across the Yellow River source region. *Hydrol. Processes*, 33(13): 1835-1850. DOI:<https://doi.org/10.1002/hyp.13441>
- Li, L., Garzione, C.N., 2017. Spatial distribution and controlling factors of stable isotopes in meteoric waters on the Tibetan Plateau: Implications for paleoelevation reconstruction. *Earth Planet. Sci. Lett.*, 460: 302-314. DOI:<https://doi.org/10.1016/j.epsl.2016.11.046>
- 565 Li, Y.-z., Gao, Z.-j., Liu, J.-t., Wang, M., Han, C., 2021. Hydrogeochemical and isotopic characteristics of spring water in the Yarlung Zangbo River Basin, Qinghai-Tibet Plateau, Southwest China. *J. Mountain Sci.*, 18(8): 2061-2078. DOI:[10.1007/s11629-020-6625-y](https://doi.org/10.1007/s11629-020-6625-y)
- 570 Li, Y., Yang, J., Tan, L., Duan, F., 1999. Impact of tectonics on alluvial landforms in the Hexi Corridor, Northwest China. *Geomorphology*, 28(3): 299-308. DOI:[https://doi.org/10.1016/S0169-555X\(98\)00114-7](https://doi.org/10.1016/S0169-555X(98)00114-7)
- Lin, X. et al., 2022. The Formation of the North Qilian Shan through Time: Clues from Detrital Zircon Fission-Track Data from Modern River Sediments. *Geosciences*, 12(4): 166.
- Ma, L., Cheng, W., Bo, J., Li, X., Gu, Y., 2018. Spatio-Temporal Variation of Land-Use Intensity from a Multi-Perspective—Taking the Middle and Lower Reaches of Shule River Basin in China as an Example. *Sustainability*, 10(3): 771.
- 575 Marandi, A., Shand, P., 2018. Groundwater chemistry and the Gibbs Diagram. *Appl. Geochem.*, 97: 209-212. DOI:<https://doi.org/10.1016/j.apgeochem.2018.07.009>
- Meng, K., Wang, E., Chu, J.J., Su, Z., Fan, C., 2020. Late Cenozoic river system reorganization and its origin within the Qilian Shan, NE Tibet. *J. Struct. Geol.*, 138: 104128. DOI:<https://doi.org/10.1016/j.jsg.2020.104128>
- 580 Meybeck, M., 1987. Global chemical weathering of surficial rocks estimated from river dissolved loads. *Am. J. Sci.*, 287(5): 401-428.
- Négrel, P., Petelet-Giraud, E., Barbier, J., Gautier, E., 2003. Surface water-groundwater interactions in an alluvial plain: Chemical and isotopic systematics. *J. Hydrol.*, 277(3-4): 248-267. DOI:[http://dx.doi.org/10.1016/S0022-1694\(03\)00125-2](http://dx.doi.org/10.1016/S0022-1694(03)00125-2)



- Paces, J.B., Wurster, F.C., 2014. Natural uranium and strontium isotope tracers of water sources and surface water–
585 groundwater interactions in arid wetlands – Pahranaagat Valley, Nevada, USA. *J. Hydrol.*, 517: 213-225.
DOI:<https://doi.org/10.1016/j.jhydrol.2014.05.011>
- Prakash Rai, S., Venyo Akpataku, K., Noble, J., Patel, A., Kumar Joshi, S., 2023. Hydrochemical evolution of groundwater in
northwestern part of the Indo-Gangetic Basin, India: A geochemical and isotopic approach. *Geosci. Front.*, 14(6): 101676.
DOI:<https://doi.org/10.1016/j.gsf.2023.101676>
- 590 Qu, B., Zhang, Y., Kang, S., Sillanpää, M., 2017. Water chemistry of the southern Tibetan Plateau: an assessment of the
Yarlung Tsangpo river basin. *Environ. Earth Sci.*, 76(2): 74. DOI:10.1007/s12665-017-6393-3
- Raymond, P.A., Oh, N.-H., Turner, R.E., Broussard, W., 2008. Anthropogenically enhanced fluxes of water and carbon from
the Mississippi River. *Nature*, 451(7177): 449-452. DOI:10.1038/nature06505
- Rehman Qaisar, F.U. et al., 2018. Spatial variation, source identification, and quality assessment of surface water geochemical
595 composition in the Indus River Basin, Pakistan. *Environ. Sci. Pollut. Res.*, 25(13): 12749-12763. DOI:10.1007/s11356-018-
1519-z
- Wang, L., Dong, Y., Xie, Y., Chen, M., 2023. Hydrological processes and water quality in arid regions of Central Asia: insights
from stable isotopes and hydrochemistry of precipitation, river water, and groundwater. *Hydrogeology Journal*.
DOI:10.1007/s10040-023-02654-1
- 600 Wang, L. et al., 2016. Distinct groundwater recharge sources and geochemical evolution of two adjacent sub-basins in the
lower Shule River Basin, northwest China. *Hydrogeology Journal*, 24(8): 1967.
- Wang, L., Dong, Y., Xu, Z., 2017. A synthesis of hydrochemistry with an integrated conceptual model for groundwater in the
Hexi Corridor, northwestern China. *J. Asian Earth Sci.*, 146(3): 20-29. DOI:<http://doi.org/10.1016/j.jseaes.2017.04.023>
- Wang, L., Li, G., Dong, Y., Han, D., Zhang, J., 2015. Using hydrochemical and isotopic data to determine sources of recharge
605 and groundwater evolution in an arid region: a case study in the upper–middle reaches of the Shule River basin, northwestern
China. *Environ. Earth Sci.*, 73(4): 1-15. DOI:10.1007/s12665-014-3719-2
- Wang, L., Liu, W., Xu, Z., Zhang, J., 2022. Water sources and recharge mechanisms of the Yarlung Zangbo River in the
Tibetan Plateau: Constraints from hydrogen and oxygen stable isotopes. *J. Hydrol.*, 614: 128585.
DOI:<https://doi.org/10.1016/j.jhydrol.2022.128585>
- 610 Wang, N. et al., 2009. Tracing the major source area of the mountainous runoff generation of the Heihe River in northwest
China using stable isotope technique. *Chin. Sci. Bull.*, 54(16): 2751-2757. DOI:10.1007/s11434-009-0505-8
- Wu, H., Wu, J., Li, J., Fu, C., 2020. Spatial variations of hydrochemistry and stable isotopes in mountainous river water from
the Central Asian headwaters of the Tajikistan Pamirs. *CATENA*, 193: 104639.
DOI:<https://doi.org/10.1016/j.catena.2020.104639>
- 615 Wu, J., Li, H., Zhou, J., Tai, S., Wang, X., 2021. Variation of Runoff and Runoff Components of the Upper Shule River in the
Northeastern Qinghai–Tibet Plateau under Climate Change. *Water*, 13(23): 3357.



- Xie, C., Zhao, L., Eastoe, C.J., Wang, N., Dong, X., 2022. An isotope study of the Shule River Basin, Northwest China: Sources and groundwater residence time, sulfate sources and climate change. *J. Hydrol.*, 612: 128043. DOI:<https://doi.org/10.1016/j.jhydrol.2022.128043>
- 620 Xie, C. et al., 2024. Spatial characteristics of hydrochemistry and stable isotopes in river and groundwater, and runoff components in the Shule River Basin, Northeastern of Tibet Plateau. *J. Environ. Manage.*, 349: 119512. DOI:<https://doi.org/10.1016/j.jenvman.2023.119512>
- Yang, H. et al., 2020a. A Regionally Evolving Transpressional Duplex Along the Northern Margin of the Altyn Tagh Fault: New Kinematic and Timing Constraints From the Sanweishan and Nanjieshan, China. *Tectonics*, 39(2): e2019TC005749. DOI:<https://doi.org/10.1029/2019TC005749>
- 625 Yang, L., Shi, Z., Zhang, S., Lee, H.F., 2020b. Climate Change, Geopolitics, and Human Settlements in the Hexi Corridor over the Last 5,000 Years. *Acta Geologica Sinica - English Edition*, 94(3): 612-623. DOI:<https://doi.org/10.1111/1755-6724.14529>
- Yang, N. et al., 2021. Hydrochemical and isotopic interpretation of interactions between surface water and groundwater in Delingha, Northwest China. *J. Hydrol.*, 598: 126243. DOI:<https://doi.org/10.1016/j.jhydrol.2021.126243>
- 630 Yin, Z., Luo, Q., Wu, J., Xu, S., Wu, J., 2021. Identification of the long-term variations of groundwater and their governing factors based on hydrochemical and isotopic data in a river basin. *J. Hydrol.*, 592: 125604. DOI:<https://doi.org/10.1016/j.jhydrol.2020.125604>
- Zhang, Z. et al., 2021. Hydrochemical characteristics and ion sources of river water in the upstream of the Shiyang River, China. *Environ. Earth Sci.*, 80(18): 614. DOI:[10.1007/s12665-021-09793-2](https://doi.org/10.1007/s12665-021-09793-2)
- 635 Zhao, Z. et al., 2001. Paleomagnetic dating of the Jiuquan Gravel in the Hexi Corridor: Implication on mid-Pleistocene uplift of the Qinghai-Tibetan Plateau. *Chin. Sci. Bull.*, 46(23): 2001-2005. DOI:[10.1007/BF02901916](https://doi.org/10.1007/BF02901916)
- Zhou, J., Ding, Y., Wu, J., Liu, F., Wang, S., 2021. Streamflow generation in semi-arid, glacier-covered, montane catchments in the upper Shule River, Qilian Mountains, northeastern Tibetan plateau. *Hydrol. Processes*, 35(8): e14276. DOI:<https://doi.org/10.1002/hyp.14276>
- 640 Zhou, J. et al., 2015. Hydrograph Separation in the Headwaters of the Shule River Basin: Combining Water Chemistry and Stable Isotopes. *Adv. Meteorol.*, 2015(1): 830306. DOI:<https://doi.org/10.1155/2015/830306>
- Zhou, J., Ding, Y., Zeng, G., Wu, J., Qin, J., 2014. Major Ion Chemistry of Surface Water in the Upper Reach of Shule River Basin and the Possible Controls. *Environmental Science*, 35(09): 3315-3324. DOI:[10.13227/j.hjxx.2014.09.011](https://doi.org/10.13227/j.hjxx.2014.09.011) (in Chinese)